Computer Networks 160 (2019) 92–104

Contents lists available at ScienceDirect

Computer Networks

journal homepage: www.elsevier.com/locate/comnet

Robust power control strategy based on hierarchical game with QoS provisioning in full-duplex femtocell networks

Zhixin Liu[a,*], Guochen Hou[a], Yang Liu[b], Xinbin Li[a], Xinping Guan[c]

[a] School of Electrical Engineering, Yanshan University, Qinhuangdao, Hebei 066004, China
[b] State Key Laboratory of Networking and Switching Technology, Beijing University of Posts and Telecommunications, Beijing, 100876, China
[c] School of Electronic, Information and Electrical Engineering, Shanghai Jiaotong University, Shanghai 200240, China

ARTICLE INFO

Article history:
Received 2 July 2018
Revised 6 May 2019
Accepted 11 June 2019
Available online 11 June 2019

Keywords:
Full duplex communications
Robust power control
Hierarchical game
QoS

ABSTRACT

In this paper, power control problem for full-duplex communications in two-tier femtocell networks is studied, where femtocells share the same frequency with macrocell uplink. In order to be more practical, the channel uncertainty in the real communication environment is considered, and described as probability constraints. To reduce the cross-tier and co-tier interferences among users and achieve the tradeoff of better quality of service(QoS) requirement and lower power consumption, a hierarchical game framework to allocate power is formulated. According to different design objectives, marginal utility and the symbol error rate (SER) are guaranteed in uplink, and transmission rate and delay are guaranteed in downlink. The utility of both uplink and downlink users are maximized. The Lagrangian method and sub-gradient method are used to solve the optimization problem and determine the optimal solution, respectively. A power iteration algorithm to achieve game equilibrium is provided. The simulation results show that the proposed algorithm behaves better performance in aspect of convergence, robustness and QoS provisioning.

1. Introduction

In recent years, the exponential growth of smart phones and mobile services has led to an increasing demand for high data rate access, and traditional cellular networks are no longer enough to meet people's needs [1]. In order to effectively utilize the spectrum resources, increase the scope of indoor coverage, reduce operators' huge infrastructure investment and increase the quality of service (QoS) of users, a femtocell technology has been proposed [2,3]. At the same time, full duplex(FD) communication technology can be combined with femtocell. FD communication technology can send and receive information simultaneously on the same channel. Compared with half duplex communication, full duplex communication has a lot of advantages. For example, it can double the throughput of the system in theory, while the feedback delay and end to end delay are reduced, and the access mode is flexible [4–6].

Without detailed network planning, the co-channel deployment of femtocells and macrocell would cause serious interference among neighboring femtocells and/or between femtocells and macrocell. Therefore, how to manage interference and ensure the quality of service of users has become an important technological challenge. In [7,8] and [9], some interference management schemes are designed to reduce the co-tier and cross-tier interference in a cellular network. In [10] and [11], with the aid of the means for integrating the channel detection technology into the FBSs, the femtocell can dynamically utilize the spectrum resources authorized to the macrocell by detecting the surrounding communication environment, so that the inter-tier interference can be effectively suppressed.

Many existing works are devoted to interference management and put forward some solutions [3,12–15]. In [3], based on the directional antenna, a scheme for suppressing interference and improving users' QoS is proposed. In [12], the dynamic frequency planning method is used to manage the interference problem. However, in the two-tier cellular network we studied, the most important way to suppress interference is to control the transmission power of the user or the base station. The base station adjusts its transmission power according to the signal quality of the adjacent users. In [14], a new distributed power adaptive algorithm is proposed. The new idea that performance of wireless networks can be analyzed using control theory is proposed in [15], and a simple power control algorithm is designed based on the virtual Proportional-Integral (PI) controller. In [16], a power control

* Corresponding author.
E-mail addresses: lzxauto@ysu.edu.cn (Z. Liu), lixb@ysu.edu.cn (Y. Liu), liu.yang@bupt.edu.cn (X. Li), xpguan@sjtu.edu.cn (X. Guan).

https://doi.org/10.1016/j.comnet.2019.06.009
1389-1286/

algorithm is proposed that maximizes the transmission rate of the FUE while minimizing the transmission power of the FUE. However, all of the above works are based on the fixed channel parameters. In the real communication environment, the channel gain will be disturbed by other factors, so it does not conform to the real situation.

As a rapidly developing technology in the communication field in recent years, the wireless distributed network has attracted more and more attention. Game theory has great advantage of solving the problem of distributed optimization, so Ref. [17], using the theory of non-cooperative game, proposes a power control algorithm to solve the problem of distributed network optimization. In [18], a power control scheme based on Stackelberg game is used to maximize the throughput of uplink or downlink in the cellular network. References [19–21] focus the interference pricing mechanism based on Stackelberg game. In [22], the power allocation based on non-cooperative game is used to optimize the allocation of spectrum resources. However, in all of the above schemes, the system only works in half-duplex and ignores the full-duplex system.

Since the transmission power of the femtocell is small, self-interference cancellation for a full-duplex system is easier to implement, and it is feasible to integrate the full-duplex technology into the femtocells. In this way, the cellular network can send and receive signals simultaneously on the same frequency, which greatly improves the spectrum utilization. In [23], a resource allocation algorithm based on matching is proposed to increase the throughput of the full-duplex system, but the performance is not significantly improved compared with the half-duplex system. In [24], resource allocation algorithm based on Benders decomposition can suppress self interference and inter node interference, but it does not increase throughput in the system. In the above full-duplex system, there is only one femtocell in the cellular network, without considering the complex interference of multiple femtocells. In [25], an optimal power allocation problem for uplink transmission in a two-tier femtocell network is proposed using a hierarchical game framework. The considered power allocation is formulated as the game between macro users and femtocell users in the uplink, which is quite different from the game between the uplink and downlink in our study. In addition, the quality of service of each user is not guaranteed in that work. In [26], a joint price and power allocation scheme in the spectrum sharing femtocells networks was put forward based on stackelberg game. The proposed power control method does not consider robustness, i.e. the uncertain channel is not taken into consideration.

In this paper, we study the full-duplex communication in two-tier femtocell network where multiple femtocells share the spectrum resource with macrocell. We focus on robust power allocation with consideration of the uncertainty of channel state information (CSI). In the uplink, while keeping low power consumption, we try to improve the user's SINR and reduce the symbol error rate (SER). In the downlink, we aim to increase the throughput of the system as much as possible. In order to improve users' quality-of-service (QoS), we guarantee that users do not exceed the maximum delay. Through hierarchical game theory, the uplink and downlink optimization problems are jointly considered, the existence and uniqueness of Nash equilibrium are proved. The robustness and effectiveness of the proposed algorithm are validated in the simulations. The main contributions of this paper are summarized as follows:

- In two-tier femtocell network, not only cross-tier interference and self-interference in the full-duplex communication, but also inter-cell interference (between different femtocells) and intra-cell interference (between uplink users and downlink users) is considered, and a power control strategy to restrain interference is proposed.
- The probability constraint, which is practical to describe the dynamic communication environment, is introduced to deal with the uncertainty of channel state information. The hierarchical game framework is formulated to improve the quality of service, such as time delay and outage probability, both of the uplink and downlink.
- The practical distributed power control algorithm is proposed to solve the problem of robust resource optimization. The complexity of the algorithm is reduced and the convergence speed is ensured.

The rest of the paper is organized as follows. In Section II, we describe the system model and problem formulation. In Section III, we analyze the hierarchical game in detail. We propose an optimal distributed algorithm in Section IV. Then we give the simulation results and performance analysis in Section V. Finally, conclusions are drawn in Section VI.

2. System model and problem formulation

2.1. System model

In this paper, We consider a two-tier femtocell network as shown in Fig. 1. Referring to [27], there is one MBS serving one MUE, the macrocell works in the frequency division duplexing (FDD). There are n femtocells, and each FBS has M uplink femtocell users (UUE) and K downlink femtocell users (DUE). For convenience, we make $M = K$. One uplink user and one downlink user form a user pair, which works on the same channel. At the same time, OFDMA technology is used, similar to [28], in the same femtocell, different user pairs are allocated to different orthogonal subchannels, so there is no interference between different user pairs in the same femtocell. In particular, the FBS is equipped with an FD antenna for simultaneous downlink transmission and uplink reception, and all UUEs and DUEs use HD antennas to ensure low hardware complexity. In order to make more efficient use of

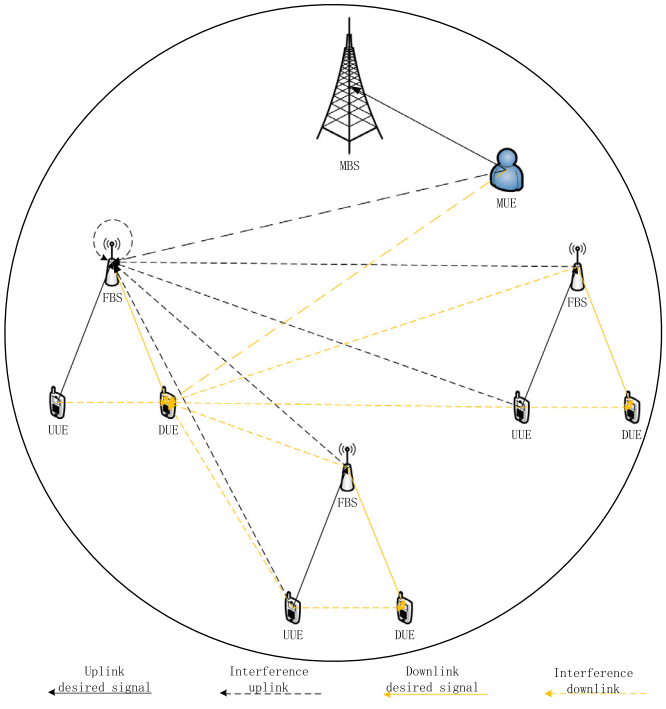

Fig. 1. System model.

spectrum resources, all FBSs can access the uplink spectrum of MBS. As shown in Fig. 1, the transmission is modeled for a given time slot. We assume all femtocells share the same frequency band with the macrocell, let B_0 and $B_i(i \in \{1, 2, \cdots, n\})$ represent MBS and the ith FBS, respectively. U_0, $U_i^u(i \in \{1, 2, \cdots, n\})$ and $U_i^d(i \in \{1, 2, \cdots, n\})$ represent the MUE, the ith UUE and the ith DUE, respectively. So, the signal-to-interference-plus-noise-ratio (SINR) of uplink can be written as [27]:

$$\gamma_i^u = \frac{g_{i,i}^u p_i^u}{g_{i,0} p_0 + \sum_{j=1}^n g_{i,j} p_j + \sum_{k=1,k\neq i}^n g_{i,k}^u p_k^u + \delta^2}. \tag{1}$$

then, the SINR of downlink can be written as:

$$\gamma_i = \frac{g_{i,i}^d p_i}{g_{i,0}^d p_0 + \sum_{l=1}^n g_{i,l}^{d,u} p_l^u + \sum_{m=1,m\neq i}^n g_{i,m}^d p_m + \delta^2}. \tag{2}$$

where p_0, p_i^u and p_i are the transmission power of U_0, U_i^u and B_i, respectively. The parameter $g_{i,0}$ is the channel gain from U_0 to B_i, $g_{i,i}^u$ is the channel gain from U_i^u to B_i, $g_{i,j}$ is the channel gain from B_j to B_i, if i is equal to j, then $g_{i,j}$ stands for self-interference. The parameter $g_{i,i}^d$ is the channel gain from B_i to U_i^d, and the parameter $g_{i,i}^{d,u}$ is the channel gain from U_i^u to U_i^d. δ^2 represents background noise in the communication environment.

2.2. Channel model

From reference [29], it can be seen that instantaneous communication links can easily change as the environment changes. Therefore, in the real communication environment, instantaneous channel state information is difficult to obtain. But we can use the average channel gain instead. In this paper, considering the Rayleigh fading communication environment, the channel gain is classified according to the network architecture, and the IMT-2000 specification is used to simplify the path loss model [30].

The outdoor-to-indoor channel gain is defined as $K_{f0} W \min(D_{i,0}^{-\alpha_{fo}}, 1)$, and the indoor channel gain is defined as $K_{fi} D_f^{-\beta}$, the channel gain from the room to the other room is defined as $K_{f0} W^2 \min(D_{i,j}^{-\alpha_{fo}}, 1)$. To simplify the channel model, the gain of the self-interference channel is set to $g_{i,i} = h_i r$, where h_i is a self-interference cancellation constant and r is a self-interference channel parameter obeying Rayleigh distribution. K_{fo} and K_{fi} represent the fixed path loss coefficient during signal transmission. W represents the partition loss during indoor-to-outdoor propagation. D represents the distance from the information sender to the receiver. β and α_{fo} represent the indoor and indoor to outdoor path loss exponents, respectively.

2.3. The uncertainty description of SINR

In this section, we deal with channel uncertainty in the real environment. In actual communication, if the channel gain is replaced with the mean value, a larger error will be brought because the channel gain is easily influenced by the environment. In this paper, we consider a sparse network deployment environment, so the interference link is less affected by the environment, and the signal link is greatly affected by the environment. Therefore, we only assume the impact of uncertain signal links on the quality of user communications. So the uplink SINR formula (1) can be rewritten as:

$$\gamma_i^u = \frac{G_{i,i}^u g_{i,i}^u p_i^u}{g_{i,0} p_0 + \sum_{j=1}^n g_{i,j} p_j + \sum_{k=1,k\neq i}^n g_{i,k}^u p_k^u + \delta^2}. \tag{3}$$

then, the downlink SINR formula (2) can be rewritten as:

$$\gamma_i = \frac{G_{i,i}^d g_{i,i}^d p_i}{g_{i,0}^d p_0 + \sum_{l=1}^n g_{i,l}^{d,u} p_l^u + \sum_{m=1,m\neq i}^n g_{i,m}^d p_m + \delta^2}. \tag{4}$$

where $G_{i,i}^u$ and $G_{i,i}^d$ obey Rayleigh distribution with probability density function $p_r(x) = \frac{x}{\sigma^2} e^{-x^2/2\sigma^2}$. It is noted that the denominator of (3) and (4) is regarded as the total interference and it can be measured by the receiver, hence they are assumed to be fixed and represented by the average channel gain model.

2.4. Hierarchical game and problem formulation

In full-duplex femtocell network system, the downlink needs a higher rate than the uplink to meet the user's needs. According to different design objectives and service requirements of the uplink and downlink, we propose to deal with the power allocation problem of uplink users and downlink users with the idea of hierarchical game, in which the uplink users are leaders and the downlink users are followers. Through the above analysis, we can define the hierarchical game as:

$$\mathcal{G} = \{\mathcal{S}, \{\mathcal{P}_i^u\}, \{\mathcal{P}_i\}, \{U_i^u\}, \{U_i\}\}, \tag{5}$$

where $\mathcal{S}$ is the player set. The strategy space of the leaders (FBSs) is given by $\{\mathcal{P}_i\}$. The strategy space of the followers (UUEs) is given by $\{\mathcal{P}_i^u\}$. Moreover $\{U_i^u\}$ and $\{U_i\}$ are the utility functions sets for followers and leaders.

2.4.1. Downlink utility function

Considering the rapid development of wireless cellular networks, the demand of users for mobile devices has shifted from a simple voice demand model to a data-centric model. Therefore, compared with the uplink, the downlink needs a higher communication rate to guarantee the user's QoS. At the same time, we need to consider the low power consumption of femtocells. We therefore model the utility function for femtocell i as consisting of two parts.

$$U_i(p_i|\mathbf{p}_{-i}, \mathbf{p}_i^u) = R(\overline{\gamma}_i) - C(p_i). \tag{6}$$

Given interfering powers $\mathbf{p}_{-i}$ and $\mathbf{p}_i^u$, femtocell i obtains an individual utility $U_i(p_i|\mathbf{p}_{-i}, \mathbf{p}_i^u)$. For its own benefit, femtocell i seeks to maximize its individual data rate. At the same time, transmitting with too much power will create unacceptable interference and huge energy consumption. Consequently, it is natural to discourage femtocells from creating large power. Hence, the optimization problem for femtocell is formulated as follows.

$$\begin{aligned} \max \ & U_i = a_i \ln(1 + \overline{\gamma}_i) - b_i p_i \\ s.t. \ & \begin{cases} \Pr[\gamma_i < \Gamma_i] \le \epsilon_1, \\ \Pr[\tau_i > \tau_i^{max}] \le \epsilon_2, \\ 0 \le p_i \le p_i^{max}, \qquad i \in \{1, 2, \cdots, n\} \end{cases} \end{aligned} \tag{7}$$

where a_i and b_i are expressed as reward coefficient and penalty coefficient, respectively. And we set them as constants. Parameter $\overline{\gamma}_i$ represents the average SINR of the femtocell. Γ_i is the required minimum SINR. $\tau_i^{\max}$ is the tolerable maximum time delay. ϵ_1, ϵ_2 are the probability threshold for SINR constraint and time delay constraint, respectively. In (7), the first probabilistic constraint is used to guarantee the outage requirement, and the second is used to guarantee the time delay requirement, which is given in Eq. (8). The used channel gain in the constraints is instantaneous γ_i, which will be transformed to the deterministic ones with aid of integral transformation. However, in the objective function, we have to used the average SINR $\overline{\gamma}_i$, in order to remove the random variable and get the deterministic expression, similar processing method can be referred to [31].

Due to the large amount of traffic handled by the downlink, we are constraining the delay in order to meet the user's requirement

for low latency. By recurring to M/M/1 queuing model [32], the relationship between the expected delay τ_i and transmission rate of downlink is described as

$$\tau_i = \frac{1}{\omega_i V_i - \psi_i}, \tag{8}$$

where V_i represents the downlink transmission rate of user d_i with uncertainties, and it can be written as $V_i = \ln(1+\gamma_i)$. The packet arrival of femtocell i follows the Poisson process with respect to parameter ψ_i, the packet length takes on the exponent distribution with respect to parameter ω_i. $\tau_i^{\max}$ is the upper bound of the expected delay in data transmission for FUE i. In order to ensure the low delay of each downlink user, probability constraint needs less or equal outage probability threshold. ϵ_1, $\epsilon_2 \in (0, 1)$. From the utility function, we can intuitively see that the reward function increases as the user's transmission rate increases, and the penalty function decreases as the power decreases. Therefore, the maximum utility function can only be obtained by reducing the power of the FBS while increasing the SINR.

2.4.2. Uplink utility function

The uplink is different from the downlink and does not guarantee a very high transmission rate. It only needs the SINR to be larger than a certain threshold. Therefore, the use of downlink utility function does not apply. Similarly, the uplink utility function consists of a reward function and a penalty function.

$$U_i^u(p_i^u, \overline{\gamma}_i^u | \mathbf{p}_{-i}^u, \mathbf{p}_i) = R(\overline{\gamma}_i^u, \Gamma_i^u) - C(p_i | \mathbf{p}_{-i}^u, \mathbf{p}_i). \tag{9}$$

As for the utility function of uplink user $U_i^u (i \in \{1, 2, \cdots, n\})$, some assumptions are given as follows.

AS 1: For the ith uplink user, given fixed p_i^u, its utility $U_i^u(p_i^u, \overline{\gamma}_i^u | \mathbf{p}_{-i}^u, \mathbf{p}_i)$ is a monotonically increasing concave upward function of its SINR $\overline{\gamma}_i^u$.

AS 2: For the ith uplink user, given fixed $\overline{\gamma}_i^u$, the utility $U_i^u(p_i^u, \overline{\gamma}_i^u | \mathbf{p}_{-i}^u, \mathbf{p}_i)$ is a monotonically decreasing concave downward function of its transmission power p_i^u.

Assumption 1 models declining satisfaction (marginal utility) obtained by uplink user i, once its current SINR $\overline{\gamma}_i^u$ exceeds Γ_i^u. Assumption 2 models increasing penalty incurred by uplink user i for causing more interference. Under assumptions 1 and 2, it can be concluded that

$$\frac{\partial U_i^u}{\partial \overline{\gamma}_i^u} > 0 \Rightarrow \frac{dR}{d\overline{\gamma}_i^u} > 0, \quad \frac{\partial U_i^u}{\partial p_i^u} < 0 \Rightarrow \frac{dC}{dp_i^u} < 0. \tag{10}$$

$$\frac{\partial^2 U_i^u}{\partial \overline{\gamma}_i^{u2}} < 0 \Rightarrow \frac{d^2R}{d\overline{\gamma}_i^{u2}} < 0, \quad \frac{\partial^2 U_i^u}{\partial p_i^{u2}} < 0 \Rightarrow \frac{d^2C}{dp_i^{u2}} \le 0. \tag{11}$$

We can reconstruct the uplink utility function as:

$$\max \ U_i^u = 1 - e^{-c_i^u(\overline{\gamma}_i^u - \Gamma_i^u)} - \frac{d_i^u}{I_i^u} p_i^u. \tag{12}$$

Assuming c_i^u, $d_i^u > 0$, it can be verified that the above choice of $R(\overline{\gamma}_i^u, \Gamma_i^u)$ and $C(p_i | \mathbf{p}_{-i}^u, \mathbf{p}_i)$ satisfies the conditions outlined in (10) and (11).

$$\frac{dR}{d\overline{\gamma}_i^u} = c_i^u e^{-c_i^u(\overline{\gamma}_i^u - \Gamma_i^u)} > 0, \ \frac{dC}{dp_i^u} = -\frac{d_i^u}{I_i^u} < 0, \tag{13}$$

$$\frac{d^2R}{d\overline{\gamma}_i^{u2}} = -c_i^{u2} e^{-c_i^u(\overline{\gamma}_i^u - \Gamma_i^u)} < 0, \ \frac{d^2C}{dp_i^{u2}} = 0. \tag{14}$$

Finally, the problem of the uplink can be expressed as

$$\max \ U_i^u = 1 - e^{-c_i^u(\overline{\gamma}_i^u - \Gamma_i^u)} - \frac{d_i^u}{I_i^u} p_i^u$$
$$s.t. \ \begin{cases} \Pr[\gamma_i^u < \Gamma_i^u] \le \epsilon_3, \\ \Pr[\eta_i^u < \eta_i^{u\min}] \le \epsilon_4, \\ 0 \le p_i^u \le p_i^{u\max}, \qquad i \in \{1, 2, \cdots, n\} \end{cases} \tag{15}$$

where c_i^u and d_i^u are expressed as reward coefficient and penalty coefficient, respectively. And we set them as constants. Parameter $\overline{\gamma}_i^u$ represents the average SINR of the ith UUE. Similar to the processing method for downlink, the average SINR is used in the objective function of uplink user. Γ_i^u is the minimum SINR of the ith UUE. Parameter I_i^u represents interference and its value is $g_{i,0}p_0 + \sum_{j=1}^n g_{i,j}p_j + \sum_{k=1,k\neq i}^n g_{i,k}^u p_k^u + \delta^2$.

Formula $\Pr[\gamma_i^u < \Gamma_i^u]$ represents the probability of $\gamma_i^u < \Gamma_i^u$. ϵ_3 is the outage probability threshold. In order to have a good SINR, the value of ϵ_3 should be small. There is co-channel interference, especially in complex communications environments, which may lead to a decrease in the reliability of data transmission. So, the concept of*SER* is introduced, denoted as $SER = 1 - \eta_i^u$, where η_i^u is the probability of successful transmission at uplink. In Rayleigh fading channels, the probability of successful transmission is related to the target SINR Γ_i^{uth} and actual SINR γ_i^u. For that γ_i^u has positive exponent correlation with the probability of successful transmission η_i^u, we approximate the probability of successful transmission as $\eta_i^u = e^{-\Gamma_i^{uth}/\gamma_i^u}$, $i \in \{1, 2, \cdots, n\}$. Formula $\Pr[\eta_i^u < \eta_i^{u\min}]$ represents the probability of $\eta_i^u < \eta_i^{u\min}$. ϵ_4 indicates the outage probability value.

From the uplink utility function, we can see that the reward function increases with the increase of SINR. The exponential reward intuitively models uplink users desire for higher SINR, which is larger than the minimum SINR target. The change of the penalty function is related to two factors. One is that the penalty function decreases with the decrease of power p_i^u, and the other is reduced with the increase of other interference I_i^u. In other word, we can not only reduce the power consumption, but also reduce the penalty by increasing the interference of the uplink itself, so that the marginal utility of the uplink is more prominent.

3. Hierarchical game analysis

3.1. Game equilibrium

Definition 1. Let p_i^* be a solution for optimization problem (7) and p_i^{u*} be a solution for problem (15). Then, if and only if for any $(\mathbf{p}_i, \mathbf{p}_i^u)$, the following conditions are satisfied:

$$U_i(p_i^*, \mathbf{p}_{-i}^*, \mathbf{p}_i^{u*}) \ge U_i(p_i, \mathbf{p}_{-i}^*, \mathbf{p}_i^{u*}), \tag{16}$$

$$U_{ui}(p_i^{u*}, \mathbf{p}_{-i}^{u\,*}, \mathbf{p}_i^*) \ge U_i^u(p_i^u, \mathbf{p}_{-i}^{u\,*}, \mathbf{p}_i^*), \tag{17}$$

point $(\mathbf{p}_i^*, \mathbf{p}_i^{u*})$ is called the equilibrium point of the game. The equilibrium point of stratified game can be obtained by finding the perfect Nash equilibrium(NE) solution of subgame. In this chapter, the upper and lower layers of the game are performed in a non-cooperative way. For a non-cooperative game, the NE is defined as the operating point where no player can improve its own utility by changing its own strategy unilaterally.

3.2. Solutions to the uplink

In this part, we solve the subgame problem of the uplink, and feed back the optimal results to the subgame problem of the downlink, and then solve the subgame problem of the downlink. Before solving the uplink optimization problem, we need to transform uncertain probabilistic constraint in (15). The SINR

probabilistic constraint is equivalent to (18), which is proved in detail in Appendix A.

$$\Gamma_i^u I_i^u - p_i^u g_{i,i}^u \sqrt{-2\ln(1-\epsilon_3)} \le 0. \tag{18}$$

Similarly, the equivalent deterministic expression of (15) can be achieved. The detailed proof is given in Appendix B. Then the probabilistic constraint of SER can be rewritten as:

$$\frac{-\Gamma_i^{uth} I_i^u}{\ln \eta_i^{umin}} - p_i^u g_{i,i}^u \sqrt{-2\ln(1-\epsilon_4)} \le 0. \tag{19}$$

In this way, we transform the uncertain probabilistic constraint problem into the deterministic one, the optimization problem (15) can be rewritten as

$$\max \ U_i^u = 1 - e^{-c_i^u(\overline{\gamma}_i^u - \Gamma_i^u)} - \frac{d_i^u}{I_i^u} p_i^u$$
$$s.t. \ \begin{cases} \Gamma_i^u I_i^u - p_i^u g_{i,i}^u \sqrt{-2\ln(1-\epsilon_3)} \le 0, \\ \dfrac{-\Gamma_i^{uth} I_i^u}{\ln \eta_i^{umin}} - p_i^u g_{i,i}^u \sqrt{-2\ln(1-\epsilon_4)} \le 0, \\ 0 \le p_i^u \le p_i^{umax}, \qquad i \in \{1, 2, \cdots, n\} \end{cases} \tag{20}$$

In femtocell network, each uplink user maximizes its respective utility through competition, and get the optimal transmission power of p_i^u. Next, we prove the existence of this subgame's NE.

Proposition 1. *An NE exists in the non-cooperative game, if* $\forall i \in \{1, 2, \cdots, n\}$, *the following statements are held [33].*

(1) p_i^u *is a nonempty convex and compact subset of some Euclidean space* $\mathcal{R}^N$.
(2) $U_i^u(p_i^u|\mathbf{P}_{-i}^u, \mathbf{P}_i)$ *is continuous in* $\mathbf{P}$ *and concave in* p_i^u.

Theorem 1. *A GE exists in the non-cooperative game* $\mathcal{G}$.

Proof. (1) Since the convex set is a single point or a continuous line in one-dimensional space. For the strategy $p_i^u \in [0, p_i^{u\max}]$, it is evident that $\{p_i^u\}$ is a nonempty, convex, and compact subset of Euclidean space $\mathcal{R}^N$.

(2) Obviously, $U_i^u(p_i^u|\mathbf{P}_{-i}^u, \mathbf{P}_i)$ is a continuous function about p_i^u. Next, by proving that $U_i^u(p_i^u|\mathbf{P}_{-i}^u, \mathbf{P}_i)$ is a second-order derivative of p_i^u and it is less than zero, we can get that $U_i^u(p_i^u|\mathbf{P}_{-i}^u, \mathbf{P}_i)$ is a concave function about p_i^u.

$$\frac{\partial U_i^u}{\partial p_i^u} = c_i^u \frac{g_{i,i}^u}{I_i^u} e^{-c_i^u(\overline{\gamma}_i^u - \Gamma_i^u)} - \frac{d_i^u}{I_i^u}, \tag{21}$$

$$\frac{\partial^2 U_i^u}{\partial p_i^{u2}} = -c_i^{u2} \left(\frac{g_{i,i}^u}{I_i^u}\right)^2 e^{-c_i^u(\overline{\gamma}_i^u - \Gamma_i^u)} < 0. \tag{22}$$

□

According to above equations, we can see that the second-order derivative of $U_i^u(p_i^u|\mathbf{P}_{-i}^u, \mathbf{P}_i)$ about p_i^u is less than 0, so $U_i^u(p_i^u|\mathbf{P}_{-i}^u, \mathbf{P}_i)$ is a concave function about p_i^u. According to Proposition 1, the NE exists in the lower subgame problem.

Because utility function $U_i^u(p_i^u|\mathbf{P}_{-i}^u, \mathbf{P}_i)$ is concave function about p_i^u, from ref. [34], we can see that the above subgame optimization problem is a convex optimization problem. Therefore optimization problem (20) can be expressed by Lagrangian multiplier method:

$$\begin{aligned} L_i^u(p_i^u, \nu_i^u, \mu_i^u) = {} & 1 - e^{-c_i^u(\overline{\gamma}_i^u - \Gamma_i^u)} - \frac{d_i^u}{I_i^u} p_i^u \\ & - \nu_i^u \left(\Gamma_i^u I_i^u - p_i^u g_{i,i}^u \sqrt{-2\ln(1-\epsilon_3)}\right) \\ & - \mu_i^u \left(\frac{-\Gamma_i^{uth} I_i^u}{\ln \eta_i^{umin}} - p_i^u g_{i,i}^u \sqrt{-2\ln(1-\epsilon_4)}\right). \end{aligned} \tag{23}$$

where ν_i^u and μ_i^u are Lagrangian multipliers. According to Lagrange function, the optimization problem (20) can be transformed into the following optimization problem:

$$\begin{aligned} &\max \ L_i^u(p_i^u, \nu_i^u, \mu_i^u) \\ &s.t. \ 0 \le p_i^u \le p_i^{u\max} \end{aligned} \tag{24}$$

We use gradient method to solve the above optimization problems. The sub-gradient of Lagrangian multipliers ν_i^u and μ_i^u can be expressed as:

$$\frac{\partial L_i^u(p_i^u, \nu_i^u, \mu_i^u)}{\partial \nu_i^u} = -\left(\Gamma_i^u I_i^u - p_i^u g_{i,i}^u \sqrt{-2\ln(1-\epsilon_3)}\right) \tag{25}$$

$$\frac{\partial L_i^u(p_i^u, \nu_i^u, \mu_i^u)}{\partial \mu_i^u} = -\left(\frac{-\Gamma_i^{uth} I_i^u}{\ln \eta_i^{umin}} - p_i^u g_{i,i}^u \sqrt{-2\ln(1-\epsilon_4)}\right), \tag{26}$$

then, the Lagrangian multipliers can be updated as follows:

$$\nu_i^{u(t+1)} = \left[\nu_i^{u(t)} - k_\nu^{(t)} \left(-\Gamma_i^u I_i^{u(t)} + p_i^{u(t)} g_{i,i}^u \sqrt{-2\ln(1-\epsilon_3)}\right)\right]^+, \tag{27}$$

$$\mu_i^{u(t+1)} = \left[\mu_i^{u(t)} - k_\mu^{(t)} \left(\frac{\Gamma_i^{uth} I_i^{u(t)}}{\ln \eta_i^{umin}} + p_i^{u(t)} g_{i,i}^u \sqrt{-2\ln(1-\epsilon_4)}\right)\right]^+, \tag{28}$$

where $[X]^+ = \max\{X, 0\}$, parameters $k_\nu^{(t)}$ and $k_\mu^{(t)}$ represent the step sizes of iteration, and satisfy the following conditions [33]:

$$\sum_{t=1}^{\infty} \left(k_\nu^{(t)}\right)^2 < \infty, \sum_{t=1}^{\infty} k_\nu^{(t)} = \infty, \tag{29}$$

$$\sum_{t=1}^{\infty} \left(k_\mu^{(t)}\right)^2 < \infty, \sum_{t=1}^{\infty} k_\mu^{(t)} = \infty. \tag{30}$$

Using the KKT condition, UUEs of the optimal power p_i^{u*} can be calculated by the following formula:

$$\frac{\partial L_i^u(p_i^u, \nu_i^u, \mu_i^u)}{\partial p_i^u} = 0, \tag{31}$$

The detailed derivation process is in Appendix C, so we can get the best transmission power of p_{ui}^*:

$$p_i^{u*} = \frac{I_i^{u*}}{g_{i,i}^u} \times \left(\frac{1}{c_i^u} \ln \frac{c_i^u g_{i,i}^u}{d_i^u - \nu_i^u I_i^{u*} g_{i,i}^u \sqrt{-2\ln(1-\epsilon_3)} - \mu_i^u I_i^{u*} g_{i,i}^u \sqrt{-2\ln(1-\epsilon_4)}} + \Gamma_i^u\right). \tag{32}$$

where $I_i^{u*} = g_{i,0} p_0 + \sum_{j=1}^n g_{i,j} p_j^* + \sum_{k=1,k\neq i}^n g_{i,k}^u p_k^{u*} + \delta^2$.

Theorem 2. *The Nash equilibrium is unique in the formulated game.*

Proof. In this part, we prove the uniqueness of Nash equilibrium. First, we show that the form of the UUEs best dynamic response is unique. Second, we demonstrate that the best response dynamic has an unique fixed point. Finally, based on the definition of Nash equilibrium, the optimal point of the best dynamic response is the Nash equilibrium, which is unique.

If the Nash Equilibrium Point is within the set of $(0, p_i^{u\max})$, we can get the dynamic optimal solution p_i^{u*} of the ith UUE by solving the formula (31). When the interference power $\mathbf{p}_{-i}^u$ and $\mathbf{p}_i$ are fixed, the unique optimal power value can be obtained. And the Nash equilibrium point is the solution of Formula (31). If the Nash equilibrium is not in the set $(0, p_i^{u\max})$, the user can obtain the optimal transmission power value at its boundary, that is, p_i^{u*} is 0 or $p_i^{u\max}$, which shows that the optimal response of the UUE

is unique. Through the above analysis, formula (32) can be written as:

$$p_i^{u*} = \min\left\{\left[\frac{I_i^{u*}}{g_{i,i}^u}\left(\frac{1}{c_i^u}\ln\frac{c_i^u g_{i,i}^u}{d_i^u - \nu_i^u I_i^{u*} g_{i,i}^u\sqrt{-2\ln(1-\epsilon_3)} - \mu_i^u I_i^{u*} g_{i,i}^u\sqrt{-2\ln(1-\epsilon_4)}} + \Gamma_i^u\right)\right]^+, p_i^{umax}\right\}. \tag{33}$$

Furthermore, the formulation (33) is rewritten as a power of iteration update $\mathbf{p}(t+1) = \mathbf{A}(\mathbf{p}(t))$, where $\mathbf{A}(\mathbf{p}(t))$ represents the power update strategy for UUE i. The individual power iteration update is shown as:

$$p_i^{u(t+1)} = \min\left\{\left[\frac{I_i^{u(t)}}{g_{i,i}^u}\left(\frac{1}{c_i^u}\ln\frac{c_i^u g_{i,i}^u}{d_i^u - \nu_i^{u(t)} I_i^{u(t)} g_{i,i}^u\sqrt{-2\ln(1-\epsilon_3)} - \mu_i^{u(t)} I_i^{u(t)} g_{i,i}^u\sqrt{-2\ln(1-\epsilon_4)}} + \Gamma_i^u\right)\right]^+, p_i^{umax}\right\}. \tag{34}$$

As long as the iteration step is small enough and satisfies (29) and (30), the sub-gradient algorithm can ensure that the power iteration formula (34) converges to its optimal value. By definition, the Nash equilibrium point is unique. □

3.3. Solutions to the downlink

For femtocell working in full duplex mode, every femtocell gets the maximum of its utility by competing with each other. According to the optimal power value p_i^{u*} of the uplink user we obtained in the previous chapter, we can get the optimal power value p_i^* of the downlink femtocell. Use the same solution method as uplink, the proof process is similar to Appendix A, then the uncertain probabilistic constraint can be rewritten as:

$$\Gamma_i I_i - p_i g_{i,i}^d\sqrt{-2\ln(1-\epsilon_1)} \le 0. \tag{35}$$

Similarly, we transform the probabilistic constraint of time delay in the formula (7). The detailed proof is in Appendix D, then the uncertain probabilistic constraint of time delay can be rewritten as:

$$(e^{\Psi_i} - 1)I_i - p_i g_{i,i}^d\sqrt{-2\ln(1-\epsilon_2)} \le 0. \tag{36}$$

where $\Psi_i = \frac{1}{\omega_i}(\frac{1}{\tau_i^{\max}} + \psi_i)$.

Optimization problem (7) can be rewritten as:

$$\begin{aligned}&\max\ \ U_i = a_i\ln(1+\overline{\gamma}_i) - b_i p_i\\ &s.t.\ \ \begin{cases}\Gamma_i I_i - p_i g_{i,i}^d\sqrt{-2\ln(1-\epsilon_1)} \le 0,\\ (e^{\Psi_i}-1)I_i - p_i g_{i,i}^d\sqrt{-2\ln(1-\epsilon_2)} \le 0,\\ 0 \le p_i \le p_i^{max}, \qquad i \in \{1,2,\cdots,n\}\end{cases}\end{aligned} \tag{37}$$

where $I_i = g_{i,0}^d p_0 + \sum_{l=1}^n g_{i,l}^{d,u} p_l^u + \sum_{m=1,m\neq i}^n g_{i,m}^d p_m + \delta^2$. According to Proposition 1, it is obvious that there exists Nash equilibrium point in the upper subgame problem of downlink. Similarly, optimization problem (37) can be transformed by Lagrangian multiplier method:

$$\begin{aligned}L_i(p_i,\lambda_i,\kappa_i) = {} & a_i\ln(1+\overline{\gamma}_i) - b_i p_i\\ & - \lambda_i\left[\Gamma_i I_i - p_i g_{i,i}^d\sqrt{-2\ln(1-\epsilon_1)}\right]\\ & - \kappa_i\left[(e^{\Psi_i}-1)I_i - p_i g_{i,i}^d\sqrt{-2\ln(1-\epsilon_2)}\right].\end{aligned} \tag{38}$$

where λ_i and κ_i are Lagrangian multipliers. According to Lagrange function, the optimization problem (37) can be transformed into the following optimization problem:

$$\begin{aligned}&\max\ \ L_i(p_i,\lambda_i,\kappa_i)\\ &s.t.\ \ 0 \le p_i \le p_i^{max}\end{aligned} \tag{39}$$

We use dual-gradient method to solve the above optimization problems. The sub-gradient of Lagrangian multipliers λ_i and κ_i can be expressed as:

$$\frac{\partial L_i(p_i,\lambda_i,\kappa_i)}{\partial\lambda_i} = -\left[\Gamma_i I_i - p_i g_{i,i}^d\sqrt{-2\ln(1-\epsilon_1)}\right], \tag{40}$$

$$\frac{\partial L_i(p_i,\lambda_i,\kappa_i)}{\partial\kappa_i} = -\left[(e^{\Psi_i}-1)I_i - p_i g_{i,i}^d\sqrt{-2\ln(1-\epsilon_2)}\right], \tag{41}$$

then, the Lagrange multipliers can be updated as follows:

$$\lambda_i^{(t+1)} = \left[\lambda_i^{(t)} - k_\lambda^{(t)}\left(-\Gamma_i I_i^{(t)} + p_i^{(t)} g_{i,i}^d\sqrt{-2\ln(1-\epsilon_1)}\right)\right]^+, \tag{42}$$

$$\kappa_i^{(t+1)} = \left[\kappa_i^{(t)} - k_\kappa^{(t)}\left((1-e^{\Psi_i})I_i^{(t)} + p_i^{(t)} g_{i,i}^d\sqrt{-2\ln(1-\epsilon_2)}\right)\right]^+. \tag{43}$$

where $[X]^+ = \max\{X,0\}$, $k_\lambda^{(t)}$ and $k_\kappa^{(t)}$ represent the step sizes of iteration, and satisfy the following conditions:

$$\sum_{t=1}^{\infty}\left(k_\lambda^{(t)}\right)^2 < \infty, \qquad \sum_{t=1}^{\infty} k_\lambda^{(t)} = \infty, \tag{44}$$

$$\sum_{t=1}^{\infty}\left(k_\kappa^{(t)}\right)^2 < \infty, \qquad \sum_{t=1}^{\infty} k_\kappa^{(t)} = \infty. \tag{45}$$

Using the KKT condition, DUEs of the optimal power p_i^* can be calculated by the following formula.

$$\frac{\partial L_i(p_i,\lambda,\kappa)}{\partial p_i} = 0. \tag{46}$$

The detailed derivation process is in Appendix E, so we can get the best transmission power of p_i^*.

$$p_i^* = \frac{a_i}{b_i - \lambda_i g_{i,i}^d\sqrt{-2\ln(1-\epsilon_1)} - \kappa_i g_{i,i}^d\sqrt{-2\ln(1-\epsilon_2)}} - \frac{I_i^*}{g_{i,i}^d}, \tag{47}$$

where $I_i^* = g_{i,0}^d p_0 + \sum_{l=1}^n g_{i,l}^{d,u} p_l^{u*} + \sum_{m=1,m\neq i}^n g_{i,m}^d p_m^* + \delta^2$.

Considering the power constraint $0 \le p_i \le p_i^{\max}$, the power iteration vector can be written as form of $\mathbf{p}(t+1) = \mathbf{A}(\mathbf{p}(t))$, where the element is

$$p_i^{(t+1)} = \min\left\{\left[\frac{a_i}{b_i - \lambda_i^{(t)} g_{i,i}^d\sqrt{-2\ln(1-\epsilon_1)} - \kappa_i^{(t)} g_{i,i}^d\sqrt{-2\ln(1-\epsilon_2)}} - \frac{I_i^{(t)}}{g_{i,i}^d}\right]^+, p_i^{max}\right\}. \tag{48}$$

The coordination steps of our proposed algorithm in full duplex networks are as follows.

In the uplink:

step 1. Each femtocell $i(i\in\{1,2,\cdots,n\})$ measures and broadcasts the corresponding uplink interference value I_i^u to its uplink user U_i^u.

step 2. Each uplink user $U_i^u(i\in\{1,2,\cdots,n\})$ computes its power p_i^u by (34).

step 3. Each uplink user $U_i^u(i\in\{1,2,\cdots,n\})$ updates multipliers ν_i^u and μ_i^u by (27) and (28).

In the downlink:

step 1. Each downlink user $U_i^d (i \in \{1, 2, \cdots, n\})$ measures and reports the corresponding downlink interference value I_i^d to its femtocell i.

step 2. Each femtocell $i (i \in \{1, 2, \cdots, n\})$ computes its power p_i by (48).

step 3. Each femtocell $i (i \in \{1, 2, \cdots, n\})$ updates multipliers $\lambda_i^{(t+1)}$ and $\kappa_i^{(t+1)}$ by (42) and (43).

Repeat the above process until power converges.

4. Optimal distributed algorithm

Through the above analysis, we can get the power iterations of both the uplink user and femtocell. With the update of the power, their respective multipliers μ_i^u, ν_i^u, λ_i and κ_i are also updated. The whole iteration operation is shown in Algorithm 1. First, the ith uplink user updates the power p_i^u according to formula (34), and then updates multipliers according to formula (27) and (28). In the downlink, the femtocell gets the updated power information of the uplink user, substitutes the information into Eq. (48) to update the ith femtocell power p_i, and then updates the multiplier λ_i and κ_i. Finally, bringing femtocell updated information to the iterative of uplink user i. Circulate the above process until all converges. It is noted that the step size k_μ, k_ν, k_λ and k_κ determine the convergence speed of the Algorithm 1. To prevent the numerical oscillation caused by too large step size value, we set the step size relatively small.

Algorithm 1 Distributed power control algorithm.

1: Input initial power value of p_i^u, p_i.
2: Initialization
- Set $t = 1$, $T = 20$, $p_i^{u(0)}$ and $p_i^{(0)}$ be any feasible point in feasible set
  $0 \le p_i^{(0)} \le p_i^{\max}$, $0 \le p_i^{u(0)} \le p_i^{u\max}$.
- Set $\mu^{(0)} \ge 0$, $\nu^{(0)} \ge 0$, $\lambda^{(0)} \ge 0$, $\kappa^{(0)} \ge 0$.
- Set step size $k_\mu^{(t)} > 0$, $k_\nu^{(t)} > 0$, $k_\lambda^{(t)} > 0$, $k_\kappa^{(t)} > 0$.

3: **while** p_i^u and p_i are not converged **do**
4: **for** $\forall i \in \{1, 2, \cdots, n\}$ **do**
5: Then, compute $p_i^{u(t+1)}$ according to (34).
6: Furthermore, multipliers $\nu_i^{u(t+1)}$ and $\mu_i^{u(t+1)}$ are computed according to (27) and (28).
7: Then, compute the downlink power p_i according to (48).
8: Multipliers $\lambda_i^{(t+1)}$ and $\kappa_i^{(t+1)}$ are computed according to (42) and (43).
9: **end for**
10: Let $t = t + 1$.
11: Until $t = T$.
12: **end while**

In this paper, we use distributed algorithm, which reduces the complexity compared with centralized algorithm. So we analyze the complexity of centralized and distributed algorithms. In centralized algorithm, we need a central controller, which needs global channel state information. In this paper, a distributed power control algorithm without centralized coordination is proposed. Each base station only needs to know the local channel state information. The complexity of EACH iteration is $O(2n + 1)$, and the convergence speed is fast in simulation. Where n represents the number of uplink or downlink users. In the centralized algorithm, we need to use the macro base station as the central controller. The complexity of the algorithm is $O((2n + 1) * n)$. Therefore, the distributed algorithm can effectively reduce the complexity of the algorithm.

5. Simulation results

In this section, we present the simulation results to verify the effectiveness of the robust power control algorithm based on hierarchical game. The considered full duplex femtocell network is shown in Fig. 2, where the MBS is located at the center and provides services for a random distributed MUEs. Within the coverage of the MBS, 10 full-duplex femtocells are randomly deployed, and each FBS simultaneously provides services for an uplink user and a downlink user. The simulation parameters are list in Table 1.

Firstly, we study the convergence of the algorithm. Figs. 3 and 4 show the convergence results of power iteration for uplink users and femtocells, respectively. It can be seen from Fig. 3 the uplink power of users converges gradually after about six iterations, and the downlink power from FBS to DUE shown in Fig. 4 converges after about four iterations. It is found that the converged power of uplink and downlink users are different, the main reason is they have different objective functions and different SINR

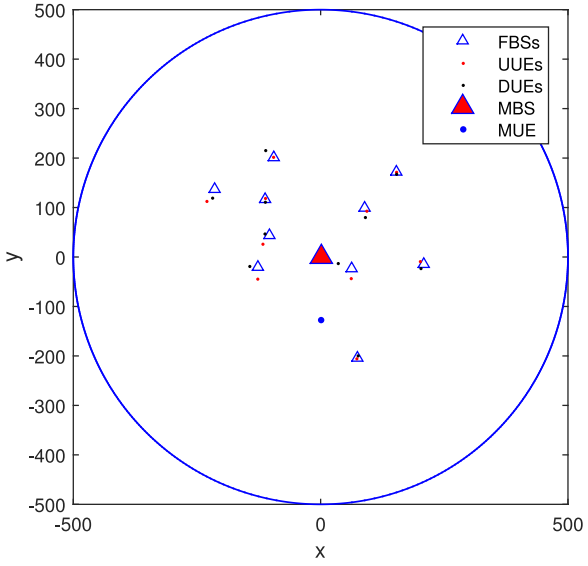

Fig. 2. Network topology.

Table 1
System parameters.

Variable	Parameter	Value
n	number of femtocell	10
R_m	macrocell radius	500 m
f	carrier frequency	2000 MHz
K_{fi}	indoor loss	$10^{3.7}$
K_{fo}	outdoor-to-indoor loss	$10^{2.8}$
W	partition loss	$10^{0.5}$
α_{fo}	outdoor path loss exponents	4
β	indoor path loss exponents	3
δ^2	mean of background noise	10^{-6}
p_0	macrocell user power	0.1 W
σ	parameter of Reyleigh distribution	1
Γ_i^u	uplink SINR threshold	0.3
Γ_i	downlink SINR threshold	25
$\eta_i^{u\,min}$	packet delivery rate threshold	0.9
τ_i^{max}	delay upper bound	10 ms
ψ_i	intensity of packet traffic	200 packets/s
ω_i	packet length	100 bits
$\epsilon_1, \epsilon_2, \epsilon_3$	outage probability threshold	0.1
ϵ_4	outage probability threshold	0.2
a_i	coefficient of rates	0.01
b_i	cost coefficients of femtocell	0.2
c_i^u	positive reward of uplink user	14
d_i^u	cost coefficients of uplink user	0.1

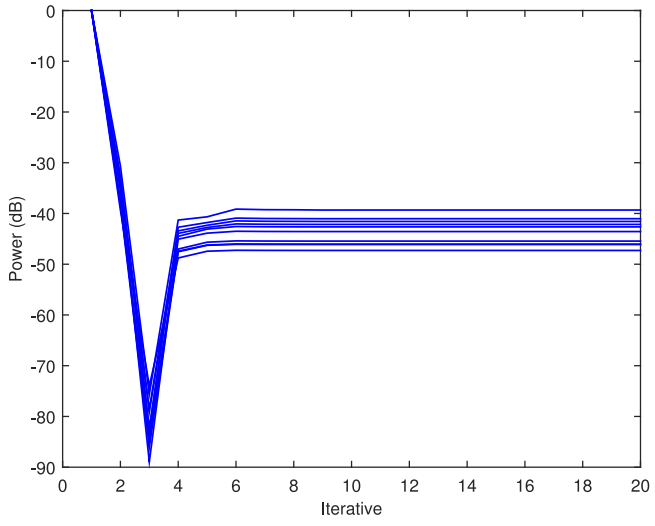

Fig. 3. Power convergence of the uplink users.

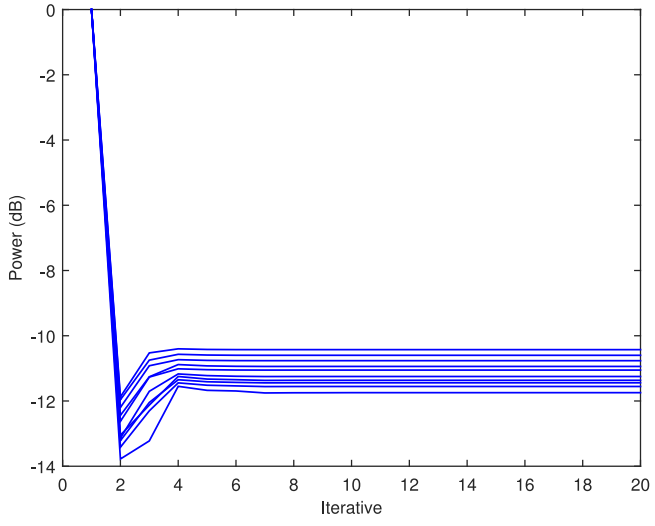

Fig. 4. Power convergence of downlink users.

thresholds. From the simulation results, the convergence speed of the proposed algorithm is fast, and the convergence is verified.

In Figs. 5 and 6, we study the constraints in the uplink. To examine the outage performance, different outage probability thresholds are given, which are 0.1, 0.2, 0.3, and 0.4 [31,35]. After obtaining the result of the power convergence, the actual outage probability value is calculated according to the formula $\Pr[\gamma_i^u < \Gamma_i^u]$, if the value is smaller than the target outage probability value, the validity of the constraint is satisfied. In this simulation, we did 1000 tests and counted the number of times less than the SINR threshold to get the actual outage probability. In Fig. 5, we give the relations between the target outage probability and the actual outage probability. From Fig. 5, we can see that the actual outage probability is less than the target outage probability, so the robustness of our proposed algorithm is satisfactory. In other words, it can better adapt to the changing environment. In Fig. 6, we study the quality of service in communication. When the user's actual SER is below our threshold, the system is stable and the user's QoS is satisfactory. It can be seen from the Fig. 6 that the SER of 10 uplink users is below the threshold of 0.1, so our power control algorithm can provide good QoS for the uplink users.

In Figs. 7 and 8, We study the constraints in the downlink. Similarly, in Fig. 7, we give the relationship between the target

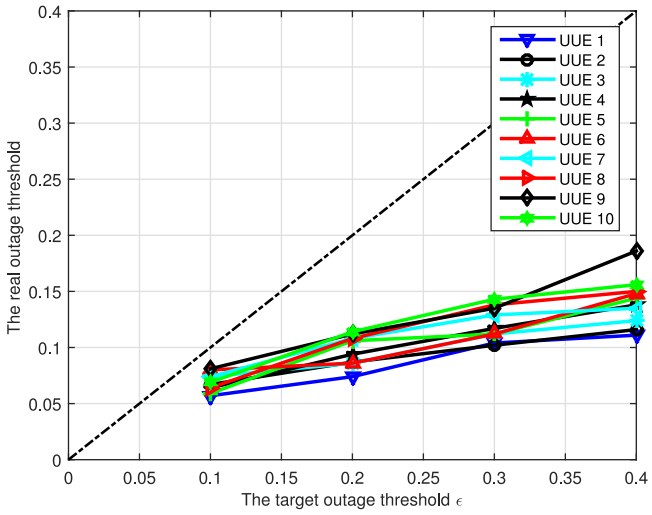

Fig. 5. Probability audit of uplink.

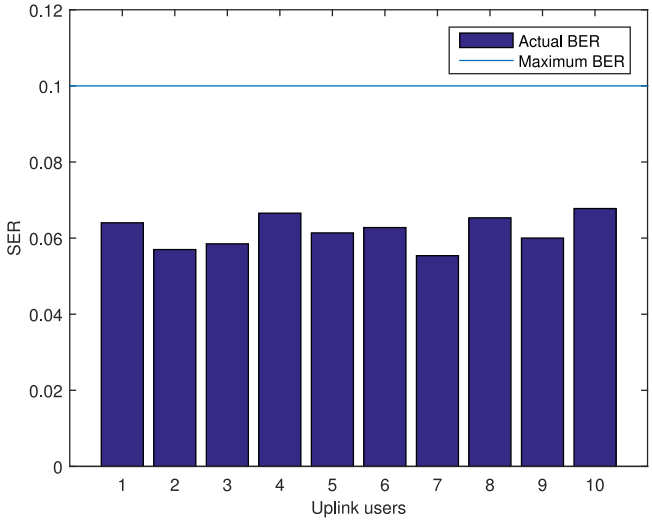

Fig. 6. User's SER of quality of service.

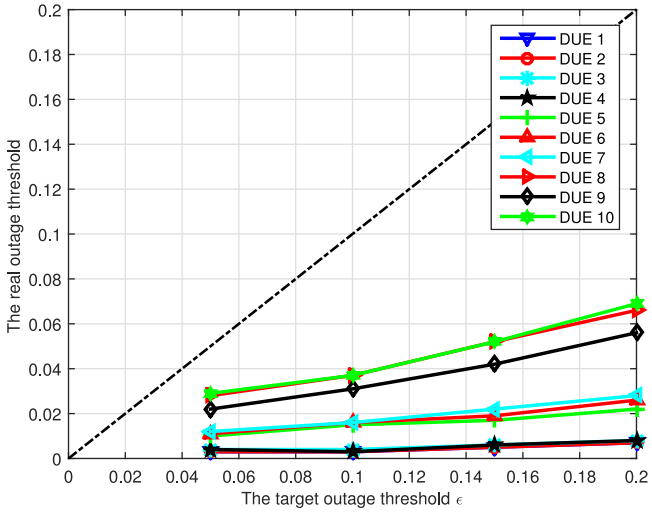

Fig. 7. Probability audit of downlink.

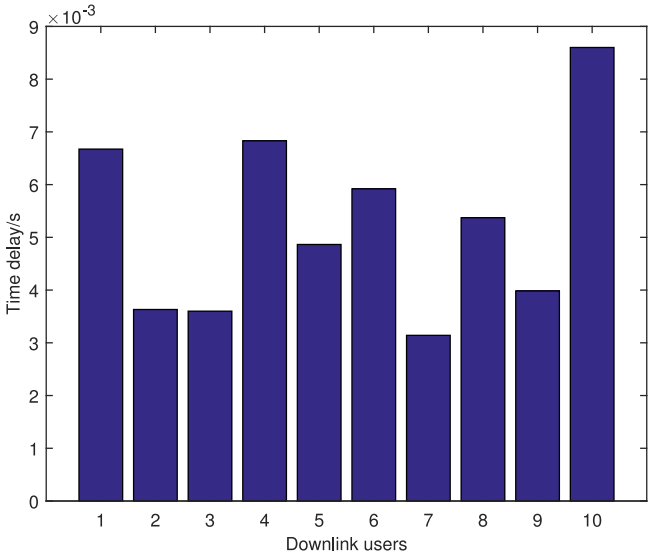

Fig. 8. User's time delay of quality of service.

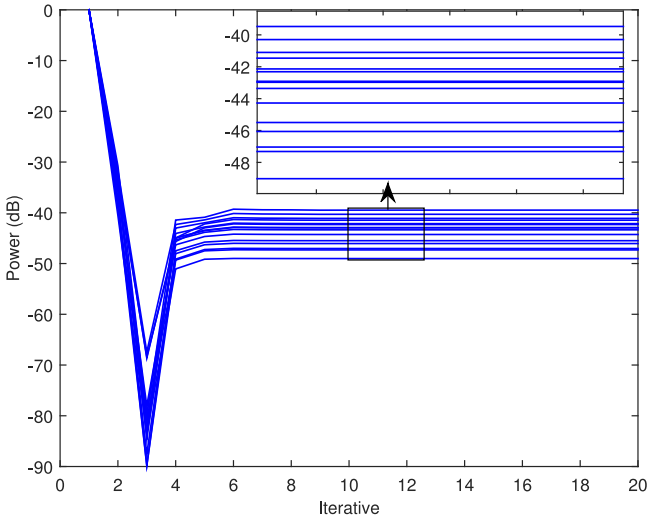

Fig. 9. Power convergence of the uplink users.

outage probability and the actual outage probability. The test was performed 1000 times. The target outage probability was set to 0.05, 0.1, 0.15, and 0.2. It can be seen from the figure that the actual outage probability is always smaller than the target outage probability, Therefore, the design requirements are satisfied and provide better robustness results. In Fig. 8, the actual value of the downlink user delay is reflected. It is found that the actual delay is under our set value 0.01 s, so our power control algorithm can provide good QoS for the downlink users.

In Figs. 9 and 10, the number of femtocells in the network topology is increased, and the convergence process of the algorithm is shown. We have increased the number of femtocells from 10 to 15 in the network, and each of the femtocells has a corresponding uplink user and downlink user operating in full-duplex mode. It can be seen that we can still get the convergence result with the increase of femtocells, and the convergence speed is the same as that of 10 femtocells.

In Figs. 11 and 12, the SINR of the algorithm is studied by increasing the number of femtocells in the network topology. In Fig. 11, we increase the number of uplink users from 10 to 15, and the SINR of each uplink user is calculated after power convergence. It can be seen that the actual SINR is greater than the SINR

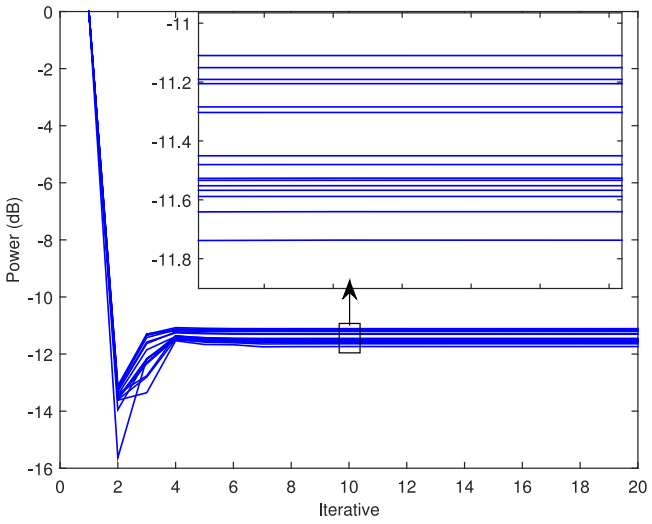

Fig. 10. Power convergence of the downlink users.

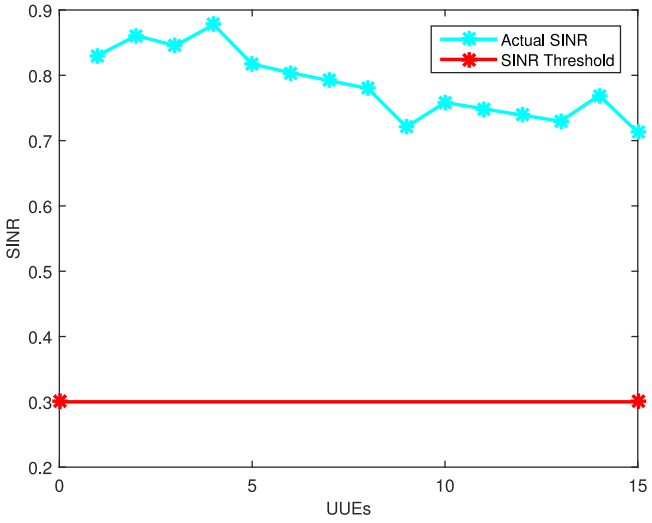

Fig. 11. SINR of uplink.

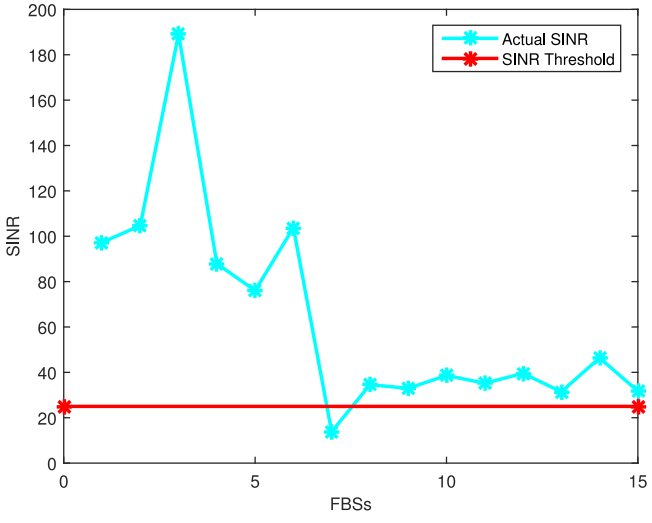

Fig. 12. SINR of downlink.

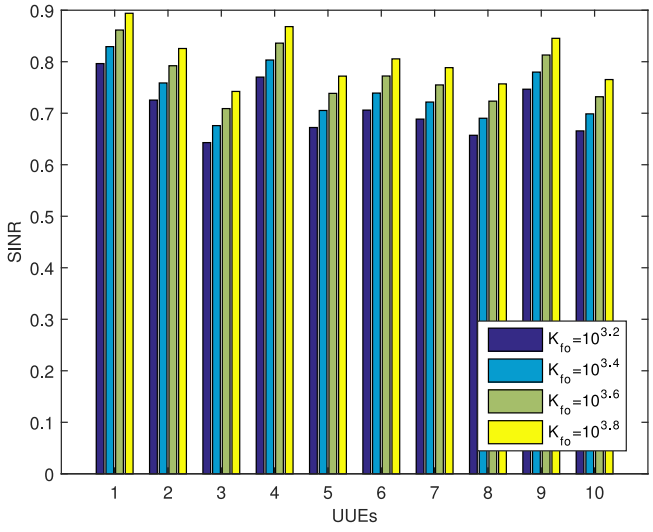

Fig. 13. SINR of uplink under different indoor losses.

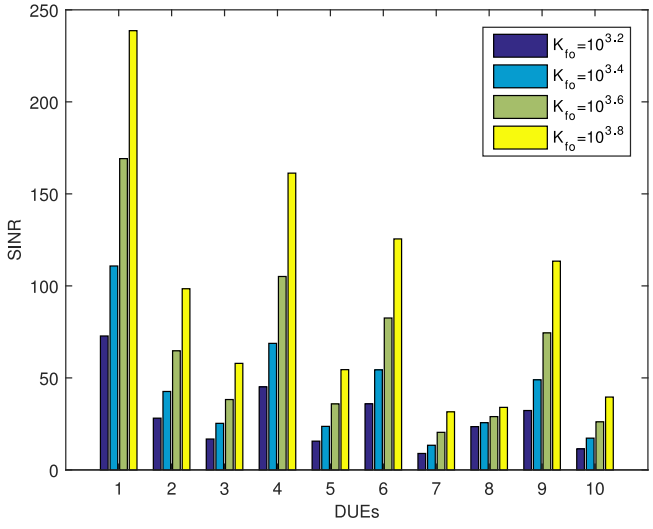

Fig. 14. SINR of downlink under different indoor losses.

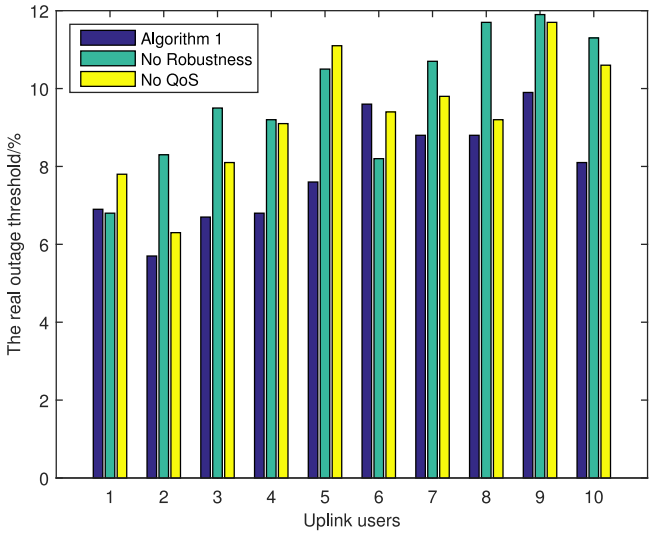

Fig. 15. Comparison in real outage percentage of UUEs with $\epsilon_3 = 0.1$.

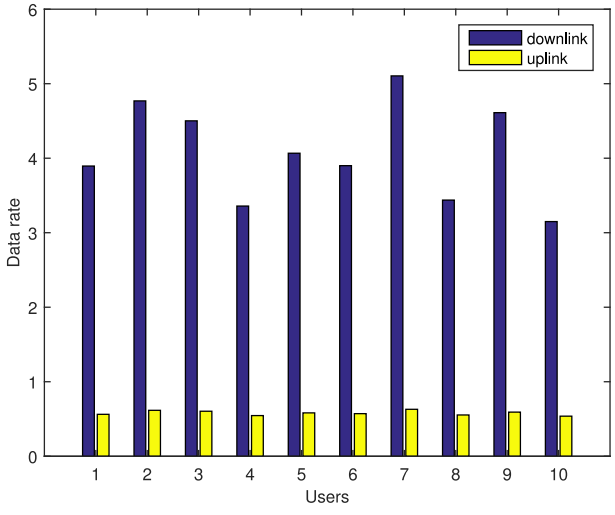

Fig. 16. Comparison of uplink and downlink transmission rates.

threshold. In Fig. 12, only the SINR of individual downlink users is less than the threshold. Therefore, we can conclude that, in the case of increasing the network topology, our algorithm can provide good QoS for the users.

Figs. 13 and 14 show the difference of SINR under different indoor losses. From the uplink and downlink, we can see that when the indoor loss is $10^{3.2}$, $10^{3.4}$, $10^{3.6}$ and $10^{3.8}$, the SINR of the uplink and downlink increases gradually with the increase of the indoor loss. In addition, with the increase of indoor loss, the link with high SINR will be more affected, while the link with smaller SINR will be less affected by the change of indoor loss.

Next, we take the part of the uplink user power control in Algorithm 1, and analyze the comparison results between Algorithm 1 and the methods in [25] and [26]. Under the same femtocell topology and channel environment, our method is compared with the method without user service quality assurance and without considering robustness. As can be seen from Fig. 15, in most users, the outage probability with Algorithm 1 is lower than that of methods without guaranteeing quality of service [25] and methods without considering the uncertain channel gains [26], and all the outage probability of users in our algorithm is lower than the threshold we set. Therefore, Algorithm 1 shows better performance in guaranteeing QoS, and has better robustness, and can better adapt to the changing environment. The uplink and downlink are with different design objectives. In the downlink, users need to provide higher transmission rates. Therefore, in Fig. 16, we compare the transmission rates of the uplink and downlink. The simulation results proved that our goal was achieved, and the transmission rate is reasonably allocated to meet users' needs.

6. Conclusions

In this paper, a full-duplex heterogeneous macrocell-femtocell network is considered. In the uplink, the marginal utility of the objective function and the user's SER are guaranteed. In the downlink, the transmission rate and low delay are ensured. A power control scheme is proposed for the uplink users and femtocells respectively, and the interference of the macrocell users in the double cellular network is also considered. The theory of hierarchical game is used to analyze the behavioral strategies between uplink and downlink. Considering the uncertain channel gain and user's QoS, the algorithm's robustness and user's satisfaction are enhanced. The simulation results show that the outage probability of uplink and downlink is lower than the threshold, and the robustness against the uncertain channel gains is guaranteed. The

the convergence of the hierarchical game and the effectiveness of the algorithm are verified.

Disclosure of conflicts of interest

The authors declare that they do not have any commercial or associative interest that represents a conflict of interest in connection with the work submitted.

Acknowledgments

This work was supported in part by the National Natural Science Foundation of China under grant no. 61873223 and no. 61602038, the Natural Science Foundation of Hebei Province under grant no. F2017203140.

Appendix A

Proof. Bring Formula (3) into the probability constraint of SINR in formula (15), we know that

$$\Pr\left[\frac{G_{i,i}^u g_{i,i}^u p_i^u}{g_{i,0}p_0+\sum_{j=1}^n g_{i,j}p_j+\sum_{k=1,k\neq i}^n g_{i,k}^u p_k^u+\delta^2}<\Gamma_i^u\right]\le\epsilon_3. \tag{49}$$

For convenience, we make

$$I_i^u=g_{i,0}p_0+\sum_{j=1}^n g_{i,j}p_j+\sum_{k=1,k\neq i}^n g_{i,k}^u p_k^u+\delta^2. \tag{50}$$

where $G_{i,i}^u$ obeys Rayleigh distribution with parameter $\sigma=1$, therefore the probability density function of $G_{i,i}^u$ is

$$f_G(x)=xe^{-\frac{1}{2}x^2}. \tag{51}$$

Then, the equivalent form of the constraint $\Pr[\gamma_i^u<\Gamma_i^u]\le\epsilon_3$ is rewritten as:

$$\begin{aligned}\Pr\left[G_{i,i}^u<\frac{\Gamma_i^u I_i^u}{g_{i,i}^u p_i^u}\right]&\le\epsilon_3\\ &\Rightarrow\int_0^{\frac{\Gamma_i^u I_i^u}{g_{i,i}^u p_i^u}}xe^{-\frac{1}{2}x^2}\mathrm{d}x\le\epsilon_3,\\ &\Rightarrow 1-e^{-\frac{1}{2}\left(\frac{\Gamma_i^u I_i^u}{g_{i,i}^u p_i^u}\right)^2}\le\epsilon_3,\\ &\Rightarrow\ln(1-\epsilon_3)\le-\frac{1}{2}\left(\frac{\Gamma_i^u I_i^u}{g_{i,i}^u p_i^u}\right)^2,\\ &\Rightarrow\Gamma_i^u I_i^u-p_i^u g_{i,i}^u\sqrt{-2\ln(1-\epsilon_3)}\le 0.\end{aligned} \tag{52}$$

□

Appendix B

Proof. It follows from $e^{\frac{-\Gamma_i^{uth}}{\gamma_i^u}}<\eta_i^{umin}$ that

$$e^{\frac{-\Gamma_i^{uth}I_i^u}{G_{i,i}^u p_i^u g_{i,i}^u}}<\eta_i^{u\min}, \tag{53}$$

$$\Rightarrow G_{i,i}^u<\frac{-\Gamma_i^{uth}I_i^u}{p_i^u g_{i,i}^u\ln\eta_i^{u\min}}. \tag{54}$$

Then, the probability constraint $Pr[\eta_i^u<\eta_i^{umin}]\le\epsilon_4$ is rewritten as

$$Pr\left[G_{i,i}^u<\frac{-\Gamma_i^{uth}I_i^u}{p_i^u g_{i,i}^u\ln\eta_i^{u\min}}\right]\le\epsilon_4. \tag{55}$$

According to the probability density function $f_{G_{i,i}^u}(x)=xe^{-\frac{1}{2}x^2}$, we have

$$\begin{aligned}\int_0^{\frac{-\Gamma_i^{uth}I_i^u}{p_i^u g_{i,i}^u\ln\eta_i^{u\min}}}xe^{-\frac{1}{2}x^2}\mathrm{d}x&\le\epsilon_4,\\ &\Rightarrow 1-e^{-\frac{1}{2}\left(\frac{-\Gamma_i^{uth}I_i^u}{p_i^u g_{i,i}^u\ln\eta_i^{u\min}}\right)^2}\le\epsilon_4,\\ &\Rightarrow\ln(1-\epsilon_4)\le-\frac{1}{2}\left(\frac{-\Gamma_i^{uth}I_i^u}{p_i^u g_{i,i}^u\ln\eta_i^{u\min}}\right)^2,\\ &\Rightarrow\frac{-\Gamma_i^{uth}I_i^u}{\ln\eta_i^{u\min}}-p_i^u g_{i,i}^u\sqrt{-2\ln(1-\epsilon_4)}\le 0.\end{aligned} \tag{56}$$

□

Appendix C

Proof. The first partial derivative of $L_i^u(p_i^u,\nu_i^u,\mu_i^u)$ to p_i^u is:

$$\begin{aligned}&\frac{\partial L_i^u(p_i^u,\nu_i^u,\mu_i^u)}{\partial p_i^u}\\ &=c_i^u\frac{g_{i,i}^u}{I_i^u}e^{-c_i^u(\overline{\gamma}_i^u-\Gamma_i^u)}-\frac{d_i^u}{I_i^u}\\ &+\nu_i^u g_{i,i}^u\sqrt{-2\ln(1-\epsilon_3)}+\mu_i^u g_{i,i}^u\sqrt{-2\ln(1-\epsilon_4)}.\end{aligned} \tag{57}$$

We make it partial derivative to 0, and we can get:

$$\begin{aligned}&c_i^u\frac{g_{i,i}^u}{I_i^u}e^{-c_i^u(\overline{\gamma}_i^u-\Gamma_i^u)}\\ &=\frac{d_i^u}{I_i^u}-\nu_i^u g_{i,i}^u\sqrt{-2\ln(1-\epsilon_3)}\\ &-\mu_i^u g_{i,i}^u\sqrt{-2\ln(1-\epsilon_4)},\\ &\Rightarrow e^{-c_i^u(\overline{\gamma}_i^u-\Gamma_i^u)}\\ &=\frac{I_i^u d_i^u-I_i^u\nu_i^u g_{i,i}^u\sqrt{-2\ln(1-\epsilon_3)}-I_i^u\mu_i^u g_{i,i}^u\sqrt{-2\ln(1-\epsilon_4)}}{c_i^u g_{i,i}^u},\\ &\Rightarrow c_i^u(\overline{\gamma}_i^u-\Gamma_i^u)\\ &=\ln\frac{c_i^u g_{i,i}^u}{I_i^u d_i^u-I_i^u\nu_i^u g_{i,i}^u\sqrt{-2\ln(1-\epsilon_3)}-I_i^u\mu_i^u g_{i,i}^u\sqrt{-2\ln(1-\epsilon_4)}},\\ &\Rightarrow\overline{\gamma}_i^u\\ &=\frac{1}{c_i^u}\ln\frac{c_i^u g_{i,i}^u}{I_i^u d_i^u-I_i^u\nu_i^u g_{i,i}^u\sqrt{-2\ln(1-\epsilon_3)}-I_i^u\mu_i^u g_{i,i}^u\sqrt{-2\ln(1-\epsilon_4)}}+\Gamma_i^u,\\ &\Rightarrow p_i^{u*}\\ &=\frac{I_i^{u*}}{g_{i,i}^u}\left(\frac{1}{c_i^u}\ln\frac{c_i^u g_{i,i}^u}{d_i^u-\nu_i^u I_i^{u*}g_{i,i}^u\sqrt{-2\ln(1-\epsilon_3)}-\mu_i^u I_i^{u*}g_{i,i}^u\sqrt{-2\ln(1-\epsilon_4)}}+\Gamma_i^u\right).\end{aligned} \tag{58}$$

□

Appendix D

Proof. It follows from $\frac{1}{\omega_i V_i-\psi_i}>\tau_i^{max}$ that

$$V_i<\frac{1}{\omega_i}\left(\frac{1}{\tau_i^{\max}}+\psi_i\right). \tag{59}$$

For convenience, we let $\Psi_i=\frac{1}{\omega_i}(\frac{1}{\tau_i^{max}}+\psi_i)$ and substitute $V_i=\ln(1+\gamma_i)$ into the formula (59)

$$\ln(1+\gamma_i)<\Psi_i,$$

$$\Rightarrow \gamma_i < e^{\Psi_i} - 1,$$
$$\Rightarrow G_{i,i}^d < \frac{(e^{\Psi_i}-1)I_i}{p_i g_{i,i}^d}. \quad (60)$$

where $I_i = g_{i,0}^d p_0 + \sum_{l=1}^{n} g_{i,l}^{d,u} p_l^u + \sum_{m=1,m\neq i}^{n} g_{i,m}^d p_m + \delta^2$, the probability constraint $\Pr[\tau_i > \tau_i^{max}] \le \epsilon_2$ is rewritten as

$$\Pr\left[G_{i,i}^d < \frac{(e^{\Psi_i}-1)I_i}{p_i g_{i,i}^d}\right] \le \epsilon_2. \quad (61)$$

According to the probability density function $f_{G_{i,i}^d}(x) = xe^{-\frac{1}{2}x^2}$, we have

$$\int_0^{\frac{(e^{\Psi_i}-1)I_i}{p_i g_{i,i}^d}} \mathrm{d}x \le \epsilon_2,$$
$$\Rightarrow 1 - e^{-\frac{1}{2}\left(\frac{(e^{\Psi_i}-1)I_i}{p_i g_{i,i}^d}\right)^2} \le \epsilon_2,$$
$$\Rightarrow \ln(1-\epsilon_2) \le -\frac{1}{2}\left(\frac{(e^{\Psi_i}-1)I_i}{p_i g_{i,i}^d}\right)^2,$$
$$\Rightarrow (e^{\Psi_i}-1)I_i - p_i g_{i,i}^d \sqrt{-2\ln(1-\epsilon_2)} \le 0.$$

□

Appendix E

Proof. The first partial derivative of $L_i(p_i, \lambda_i, \kappa_i)$ to p_i is:

$$\frac{\partial L_i(p_i,\lambda_i,\kappa_i)}{\partial p_i} = \frac{a_i g_{i,i}^d}{(1+\overline{\gamma}_i)I_i} - b_i + \lambda_i g_{i,i}^d \sqrt{-2\ln(1-\epsilon_1)} + \kappa_i g_{i,i}^d \sqrt{-2\ln(1-\epsilon_2)}. \quad (62)$$

We make it partial derivative to 0, and we can get:

$$\frac{a_i I_i}{I_i + p_i g_{i,i}^d}\frac{g_{i,i}^d}{I_i} - b_i + \lambda_i g_{i,i}^d \sqrt{-2\ln(1-\epsilon_1)} + \kappa_i g_{i,i}^d \sqrt{-2\ln(1-\epsilon_2)} = 0,$$
$$\Rightarrow \frac{a_i g_{i,i}^d}{I_i + p_i g_{i,i}^d} = b_i - \lambda_i g_{i,i}^d \sqrt{-2\ln(1-\epsilon_1)} - \kappa_i g_{i,i}^d \sqrt{-2\ln(1-\epsilon_2)},$$
$$\Rightarrow I_i + p_i g_{i,i}^d = \frac{a_i g_{i,i}^d}{b_i - \lambda_i g_{i,i}^d \sqrt{-2\ln(1-\epsilon_1)} - \kappa_i g_{i,i}^d \sqrt{-2\ln(1-\epsilon_2)}},$$
$$\Rightarrow p_i = \frac{a_i}{b_i - \lambda_i g_{i,i}^d \sqrt{-2\ln(1-\epsilon_1)} - \kappa_i g_{i,i}^d \sqrt{-2\ln(1-\epsilon_2)}} - \frac{I_i}{g_{i,i}^d}. \quad (63)$$

□

References

[1] Z. Zhang, X. Chai, K. Long, A.V. Vasilakos, Full duplex techniques for 5G networks: self-interference cancellation, protocol design, and relay selection, IEEE Commun. Mag. 53 (5) (2015) 128–137.
[2] L. Wang, F. Tian, T. Svensson, D. Feng, Exploiting full duplex for device-to-device communications in heterogeneous networks, IEEE Commun. Mag. 53 (5) (2015) 146–152.
[3] A. Mukherjee, D. De, P. Deb, Interference management in macro-femtocell and micro-femtocell cluster-based long-term evaluation-advanced green mobile network, IET Commun. 10 (5) (2016) 468–478.
[4] L. Song, Y. Li, Z. Han, Resource allocation in full-duplex communications for future wireless networks, IEEE Wireless Commun. 22 (4) (2015) 88–96.
[5] H. Ju, E. Oh, D. Hong, Catching resource-devouring worms in next-generation wireless relay systems: two-way relay and full-duplex relay, IEEE Commun. Mag. 47 (9) (2009) 58–65.
[6] D. Kim, S. Park, H. Ju, D. Hong, Transmission capacity of full-duplex-based two-way ad hoc networks with ARQ protocol, IEEE Trans. Veh. Technol. 63 (7) (2014) 3167–3183.
[7] A. Abdelnasser, E. Hossain, I.K. Dong, Clustering and resource allocation for dense femtocells in a two-tier cellular OFDMA network, IEEE Trans. Wireless Commun. 13 (3) (2014) 1628–1641.
[8] I.S. Cho, S.J. Baek, Distributed power allocation for femtocell networks subject to macrocell SINR balancing, IEEE Commun. Lett. 20 (11) (2016) 2296–2299.
[9] Y.S. Liang, W.H. Chung, G.K. Ni, I.Y. Chen, H. Zhang, S.Y. Kuo, Resource allocation with interference avoidance in OFDMA femtocell networks, IEEE Trans. Veh. Technol. 61 (5) (2012) 2243–2255.
[10] Z. Liu, J. Wang, Y. Xia, R. Fan, H. Jiang, H. Yang, Power allocation robust to time-varying wireless channels in femtocell networks, IEEE Trans. Veh. Technol. 65 (4) (2016) 2806–2815.
[11] H. Park, T. Hwang, Energy-efficient power control of cognitive femto users for 5G communications, IEEE J. Sel. Areas Commun. 34 (4) (2016) 772–785.
[12] S. Lin, W. Ni, H. Tian, R.P. Liu, An evolutionary game theoretic framework for femtocell radio resource management, IEEE Trans. Wireless Commun. 14 (11) (2015) 6365–6376.
[13] K. Senel, M. Akar, Performance analysis of a distributed power control algorithm for shared and split spectrum femtocell networks, Control Theory Technol. 14 (4) (2016) 314–322.
[14] K. Senel, M. Akar, A distributed coverage adjustment algorithm for femtocell networks, IEEE Trans. Veh. Technol. 66 (2) (2017) 1739–1747.
[15] Z. Liu, Y. Yuan, H. Yuan, X. Guan, Power allocation based on proportional-integral controller in femtocell networks with consideration of maximum power constraint, IEEE Syst. J. 13 (1) (2019) 88–97.
[16] M.R. Mili, K.A. Hamdi, F. Marvasti, M. Bennis, Joint optimization for optimal power allocation in OFDMA femtocell networks, IEEE Commun. Lett. 20 (1) (2016) 133–136.
[17] I. Ahmad, S. Liu, Z. Feng, Q. Zhang, P. Zhang, Price based spectrum sharing and power allocation in cognitive femtocell network, in: IEEE Vehicular Technology Conference, 2013, pp. 1–5.
[18] K. Xin, Z. Rui, M. Motani, Price-based resource allocation for spectrum-sharing femtocell networks: a stackelberg game approach, IEEE J. Sel. Areas Commun. 30 (3) (2012) 538–549.
[19] Z. Liu, L. Hao, Y. Xia, X. Guan, Price bargaining based on the stackelberg game in two-tier orthogonal frequency division multiple access femtocell networks, IET Commun. 9 (1) (2014) 133–145.
[20] Z. Liu, S. Li, K. Ma, X. Guan, X. Li, Robust power allocation based on hierarchical game with consideration of different user requirements in two-tier femtocell networks, Comput. Netw. 122 (2017) 179–190.
[21] L. Li, M. Wei, C. Xu, Z. Zhou, Rate-based pricing framework in hybrid access femtocell networks, IEEE Commun. Lett. 19 (9) (2015) 1560–1563.
[22] I. Ahmad, S. Liu, Z. Feng, Q. Zhang, P. Zhang, Game theoretic approach for joint resource allocation in spectrum sharing femtocell networks, J. Commun. Netw. 16 (6) (2014) 627–638.
[23] T.T. Tran, V.N. Ha, B.L. Long, A. Girard, Uplink/downlink matching based resource allocation for full-duplex OFDMA wireless cellular networks, in: Wireless Communications and Networking Conference, 2017, pp. 1–6.
[24] D.W.K. Ng, Y. Wu, R. Schober, Power efficient resource allocation for full-duplex radio distributed antenna networks, IEEE Trans. Wireless Commun. 15 (4) (2015) 2896–2911.
[25] Q. Han, B. Yang, X. Wang, K. Ma, Hierarchical-game-based uplink power control in femtocell networks, IEEE Trans. Veh. Technol. 63 (6) (2014) 2819–2835.
[26] I. Ahmad, S. Liu, Z. Feng, Q. Zhang, P. Zhang, Game theoretic approach for joint resource allocation in spectrum sharing femtocell networks, J. Commun. Netw. 16 (6) (2014) 627–638.
[27] S. Xiao, X. Zhou, Y.W. Yi, G.Y. Li, W. Guo, Robust resource allocation in full-duplex-enabled OFDMA femtocell networks, IEEE Trans. Wireless Commun. 16 (10) (2017) 6382–6394.
[28] H. Wang, R. Song, S.H. Leung, Mitigation of uplink ICI and IBI in OFDMA two-tier networks, IEEE Trans. Veh. Technol. 65 (8) (2016) 6244–6258.
[29] S.H. Park, O. Simeone, O. Sahin, S. Shamai, Robust and efficient distributed compression for cloud radio access networks, IEEE Trans. Veh. Technol. 62 (2) (2012) 692–703.
[30] V. Chandrasekhar, J.G. Andrews, T. Muharemovic, Z. Shen, A. Gatherer, Power control in two-tier femtocell networks, IEEE Trans. Wireless Commun. 8 (8) (2009) 4316–4328.
[31] Z. Liu, S. Wang, Y. Liu, Y. Wang, Secrecy transmission for femtocell networks against external eavesdropper, IEEE Trans. Wireless Commun. 17 (8) (2018) 5016–5028.
[32] M.H. Tai, N.H. Tran, C.T. Do, S.M.A. Kazmi, E.N. Huh, C.S. Hong, Power control for interference management and QoS guarantee in heterogeneous networks, IEEE Commun. Lett. 19 (8) (2015) 1402–1405.
[33] G. Owen, Game Theory, Academic, New York, NY, USA, 2005.
[34] K. Zhu, E. Hossain, A. Anpalagan, Downlink power control in two-tier cellular OFDMA networks under uncertainties: a robust stackelberg game, IEEE Trans. Commun. 63 (2) (2015) 520–535.
[35] J. Wang, L. He, J. Song, Outage analysis for downlink NOMA with statistical channel state information, IEEE Wireless Commun. Lett. 7 (2) (2017) 142–145.

Zhixin Liu received his B.S., M.S., and Ph.D. degrees in control theory and engineering from Yanshan University, Qinhuangdao, China, in 2000, 2003, and 2006, respectively. He is currently a professor with the Department of Automation, Institute of Electrical Engineering, Yanshan University, China. He visited the University of Alberta, Edmonton, AB, Canada, in 2009. He is the author or a coauthor of more than 80 papers in technical journals and conference proceedings. His current research interests include performance optimization and energy-efficient protocol design in wireless sensor networks, wireless resource allocation in cognitive radio networks and Femtocell networks.

Guochen Hou is currently working toward the M.S. degree in the Institute of Electrical Engineering, Yanshan University, China. His current research interests include wireless resources allocation, performance optimization of Femtocell networks.

Yang Liu received the BE degree in electrical engineering and its automation and the ME degree in control theory and control engineering from Harbin Engineering University, Harbin, China, in 2008 and 2010, respectively, and the Ph.D degree in computer engineering at the Center for Advanced Computer Studies, University of Louisiana at Lafayette, Lafayette, in 2014. He is currently an assistant professor at Beijing University of Posts and Telecommunications. His current research interests include wireless networking and mobile computing. He is a member of the IEEE and ACM.

Xinbin Li received his M.S. Degree in Control Theory and Control Engineering from Yanshan University, China in 1999, and the Ph.D. Degree in General and Fundamental Mechanics from Peking University, China in 2004. He is now a professor in the Institute of Electrical Engineering, Yanshan University, China. His research interests include nonlinear system and femtocell networks.

Xinping Guan received his B.S. degree in mathematics from Harbin Normal University, Harbin, China, in 1986 and his M.S. degree in applied mathematics and his Ph.D. degree in electrical engineering from the Harbin Institute of Technology in 1991, and 1999, respectively. He is currently a Professor with the Department of Automation, School of Electronic, Information, and Electrical Engineering, Shanghai Jiao Tong University, Shanghai, China. He is the author or a coauthor of more than 100 papers in mathematical and technical journals and conference proceedings. As an investigator or co-investigator, he has finished more than 20 projects supported by the National Natural Science Foundation of China (NSFC), the National Education Committee Foundation of China, and other important foundations. His current research interests include wireless sensor networks, congestion control of networks, robust control and intelligent control for nonlinear systems, chaos control, and synchronization. Prof. Guan received a Special Appointment Professorship under the CheungKong Scholars Program by the Ministry of Education of China in 2005 and the National Science Fund for Distinguished Young Scholars of China in 2005. He became a Fellow of IEEE in 2017.